Mode Conversion, Current Drive and Flow Drive with High Power ICRF Waves in Alcator C-Mod: Experimental Measurements and Modeling

M. Porkolab, P.T. Bonoli, L. Lin, Y. Lin, E. Nelson-Melby,[1] A. Parisot, J.E. Rice, G. Schilling,[2] J.C. Wright, and S.J. Wukitch

MIT Plasma Science and Fusion Center, Cambridge MA 02139 USA
Email: porkolab@psfc.mit.edu
[1]present address Pima Community College, Tucson AZ USA
[2]Princeton Plasma Physics Laboratory, Princeton NJ 08543 USA

Abstract. Recent results from high power ion cyclotron heating experiments (ICRF) in the Alcator C-Mod tokamak are reported. In particular, mode converted waves in the vicinity of the ion-ion hybrid layer have been measured by means of Phase Contrast Imaging techniques (PCI). The measured k-spectrum and spatial location of the waves is in agreement with theoretical predictions as well as with the full-wave TORIC code modeling results. For appropriate ion species (i.e., H-He3 in C-Mod, which is equivalent to DT in ITER), in tokamak geometry mode-conversion of the fast magnetosonic wave into the electromagnetic ion cyclotron waves (ICW) dominates over ion Bernstein waves (IBW). The waves propagate back toward the antenna on the low field side, in contrast to what is expected for IBW wave propagation. Experimental verification of such code predictions is essential for reliable predictive capability in future burning plasma experiments (ITER). In agreement with experimental observations, the TORIC results verify that the RF power is mainly converted to the ICW rather than IBW under most scenarios, ie H(^{3}He) and D(^{3}He). Associated with the electron Landau absorption of the mode converted waves, we are predicting mode conversion current drive of the order of 100 kA at 3 MW RF power using the new improved 4-strap antenna at 90° phasing, centered at N_ϕ = 7. These experiments are in progress. Initial results indicate significant modification of the sawtooth period by such techniques. In addition, flow drive experiments are being carried out with the aim of flow stabilization of turbulence, but the results to date are inconclusive.

1.0 Introduction

Mode conversion of long wavelength fast electromagnetic (magnetosonic) waves (or simply the Fast Wave, or FW) into shorter wavelength slow electrostatic (ion-Bernstein, or IBW) or electromagnetic (ion cyclotron, or ICW) waves is of great interest in laboratory and magnetic fusion experiments [1,2,3]. These processes are particularly important in multi-ion species plasmas in the Advanced Tokamak (AT) regimes where plasma profile control can be achieved by using the present mode conversion processes as discussed below. In particular, current drive and sheared plasma flows utilizing mode converted waves are believed to be important tools to control the local plasma current profile and to suppress plasma turbulence in AT plasma regimes. In this paper, we describe results from high power ion cyclotron heating experiments in the Alcator C-Mod tokamak where mode converted waves in the vicinity of the ion-ion hybrid layer have been measured by means of Phase Contrast Imaging techniques (PCI) [4]. The measured k-spectrum and spatial location of the waves is in agreement with the theoretical predictions of Perkins [2] who showed that in a sheared magnetic field mode-conversion of the Fast Wave (FW) into ICW dominates over IBW for appropriate ion species (i.e., D-T, or equivalently, H-^{3}He in C-Mod). Recent simulations with full wave codes [4,5,6] verify the interpretation of such mode conversion processes. Experimental verification of these code predictions is essential for reliable predictive capability in future burning plasma experiments (ITER). In this paper we shall summarize both experimental observations and code predictions of mode conversion processes in the ion cyclotron range of frequencies (ICRF) in sheared magnetic fields and discuss their absorption mechanisms. In addition, mode converted waves are predicted to drive plasma current and

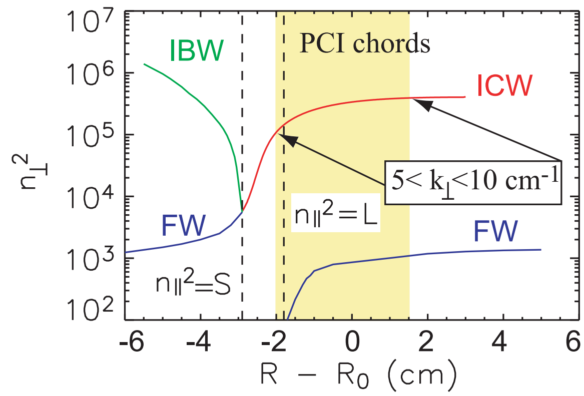

Figure 1: Dispersion relationships of the FW, IBW and ICW as a function of radial location. The dashed lines at ΔR=-3 cm correspond to the mode conversion layer, and at ΔR = -1.8 cm, to the left hand cut-off. N_ϕ = 13 and m=0. The antenna is located at the low-field side (right of 6 cm).

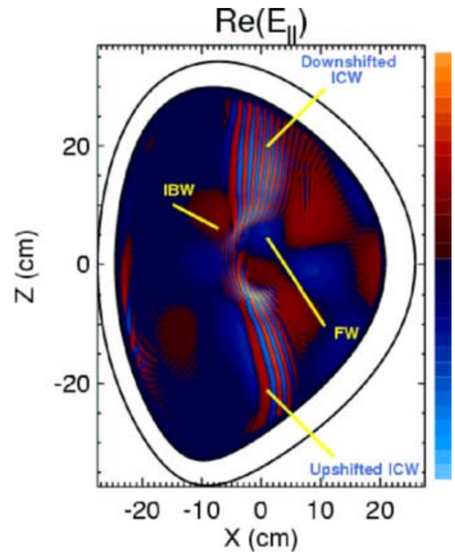

Figure 2: TORIC modeling (plasma parameters for this case are given in Sec.2).

plasma flow. We present here initial results from current drive and flow drive experiments on C-Mod and compare them with model predictions.

The physics of the mode conversion process is usually described by the following relationship [3],

$$n_\perp^2=(R- n_{\parallel}^2)(L- n_{\parallel}^2)/(S- n_{\parallel}^2),$$

where the parameters R, L, and S are the usual Stix definitions [1] and where the vanishing numerators correspond to the right ($R = n_{\parallel}^2$) and left ($L = n_{\parallel}^2$) hand cut off layers, and the mode conversion location is indicated by the vanishing of the denominator, or resonance location, $S = n_{\parallel}^2$**.** Here the hot plasma corrections become important and mode conversion of the FW into one of the slow waves is predicted (either IBW or ICW). Pictorially, these processes are depicted in Figure 1. In particular, the spatial location of the incoming fast wave, and mode converted IBW and ICW are shown where the ICW dispersion is calculated for a flux surface tangent to the mode conversion surface at r=3 cm. Numerical simulation using TORIC (see Figure 2) and the full electromagnetic dispersion relation suggest that mode conversion to IBW or ICW depends strongly upon the sheared magnetic field. High poloidal mode numbers in the mode converted wave fields are converted to large parallel wave numbers via the magnetic shear. These code results were obtained recently [5,6] using high speed computing, allowing very high resolution of mode numbers, corresponding to inverse wave numbers equal to the ion gyro-radius. The power deposition profiles obtained from either TORIC, or from a numerical solution of the hot plasma dispersion relationship in a sheared slab geometry [7] agree well and show that under typical experimental conditions electron Landau absorption of the ICW dominates. Thus, current drive or flow drive utilizing mode converted waves will be dominated by the ICW. Additional power absorption and current drive will also occur by the direct electron Landau /TTMP absorption of the FW in finite electron beta plasmas (peaking on axis where the electron temperatures are highest) and "minority" ion absorption near the cyclotron resonance layer [3].

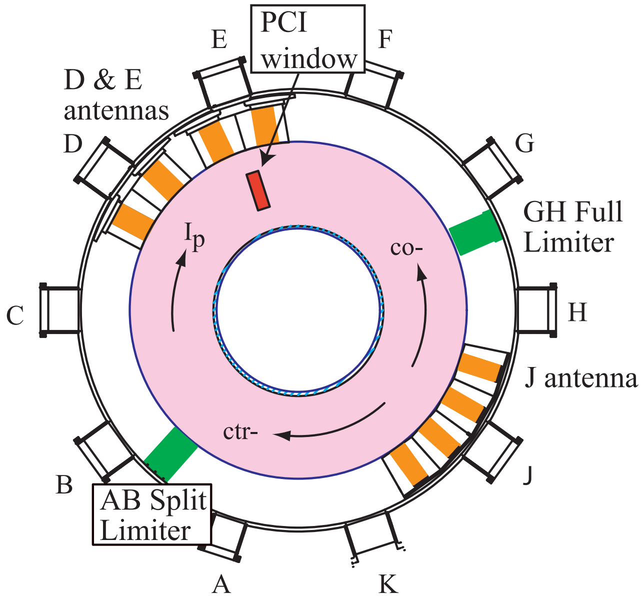

Figure 3: Top view of the C-Mod tokamak showing the location of the three antennas and the position of the wave diagnostic location. The direction of wave launch is also shown for co- and ctr-current drive antenna phasing.

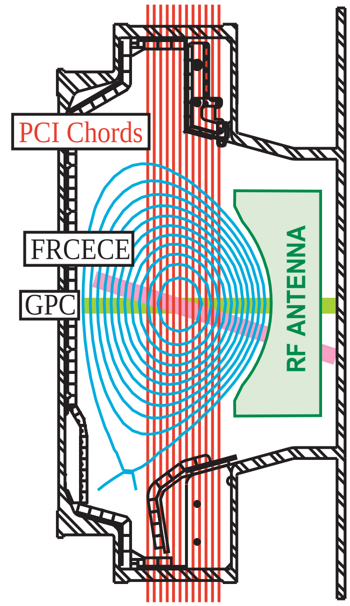

Figure 4: C-Mod poloidal cross section showing the location of the PCI cords and ECE diagnostics.

To verify mode conversion physics, a complete experimental mapping of the mode converted waves is important. This requires measuring waves of various wavelengths, 0.1-10 cm, over a wide region of plasma. The phase contrast imaging (PCI) allows the observation of a large region of the radial plasma cross-section and a wide range of wave-numbers simultaneously, although without information on vertical localization along the laser beam [4].

2.0 Experimental Setup and TORIC Description

Alcator C-Mod is a compact (major radius R = 0.67 m, minor radius a = 0.22 m), high field ($B_T \leq 8.1$ T) diverted tokamak. The discharges analyzed here are single null L-mode D(H), H(^{3}He), or D(^{3}He) minority (minority in parentheses) ICRF heated discharges. The on-axis toroidal fields, B_T, were 5.2-5.8 T and 8 T, and the plasma current, I_p, was 0.8-1 MA with the central density $\leq 2 \times 10^{20}$ m^{-3}. The ICRF heating power is coupled to the plasma via three fast wave antennas [Figure 3]. The two-strap antennas, D and E, are operated in the heating mode $(0,\pi)$ phasing, at 80 MHz and the four-strap antenna, J, is operated at 50 MHz for the 5 T discharges and 78 MHz for the 8 T discharges. This places the ^{3}He cyclotron resonance on the low field side of the magnetic axis for the 5 T discharges and near axis for the 8 T discharges. The J antenna injected up to 1.5 MW for both heating $(0,\pi,\pi,0)$ and co- and counter- current drive $(0,\pm\pi/2,\pm\pi,\pm3\pi/2)$ phasing. For the ~5 T D(H) discharges, at 78 MHz the H minority cyclotron resonance is located on the low field side, near the magnetic axis.

The primary RF wave diagnostic is a CO_2 laser based PCI diagnostic (PCI)[4,8,9]. The PCI diagnostic converts phase variation arising from density fluctuations to intensity variation through the interference of the scattered and $\lambda/4$ phase-shifted un-scattered beam passing through the plasma. The beam is imaged onto a 32 channel HgCdTe photoconductive detector. The detector is digitized at 10 MHz and the system has a frequency range of 2 kHz $< f <$ 5 MHz. The beam, typically expanded to 12-15 cm in the experiments described here, makes a vertical pass through the plasma as shown in Figure 4. For the current C-Mod PCI diagnostic, the minimum wavenumber is determined by the beam width and is typically 0.4-0.5 cm^{-1} for the experiments described herein. The maximum wavenumber is determined by the channel separation, controlled by the magnification of the image onto the detector, and is typically 8-10 cm^{-1} for the present experiments (the diagnostic is presently being upgraded to measure k_R=30 cm^{-1}). The PCI is most sensitive to waves propagating perpendicular to the beam path; therefore, the diagnostic is most sensitive to waves with significant wavenumber along the major radius (k_R). To detect density fluctuations associated RF mode converted waves at 50, 78 and 80 MHz, the laser intensity is modulated near the RF frequency. The selected modulation frequency is shifted from the RF frequency typically ≤1 MHz, for example 50.75 MHz. When the 50 MHz fluctuation in the plasma is illuminated by the 50.75 MHz modulated laser, the image intensity (which is the product of both) reveals a 750 kHz beat oscillation, the frequency at which the signal is detected.

The principal simulation tool is the finite Larmor radius (FLR) full wave code TORIC. The code has been described in detail in a number of references (see Ref. 5 for a list of previous references and history of upgrades and the paper by J. Wright et al [10] at this conference) and will be described here briefly. For a fixed frequency and toroidal mode number, TORIC solves Maxwell's equations in an axisymmetric toroidal plasma, including an antenna model, assuming a linear response using a mixed spectral-finite element basis. TORIC has been compared with AORSA [6] (an all orders full wave code) in 2-D and with METS (a 1-D all orders code) and found to be in good agreement in mode conversion scenarios[5,11]. This suggests the less computationally intensive TORIC model can accurately simulate mode conversion scenarios for C-Mod. As a result of the poloidal mode coupling in a tokamak, a large number of poloidal modes, m, are required to represent discontinuities such as mode conversion. For the current TORIC basis, the resolution requirements can be estimated from the condition that $k_\perp\rho_i \sim 1$ and $k_\perp \sim m/r$ [11]. For the C-Mod experiments discussed here, $m \leq 255$ modes is sufficient for converged solutions. In order to routinely carry out large poloidal mode simulations, TORIC has been parallelized and further improvements in the code algorithm have allowed for 255 mode simulations to become routine on an "in-house" 48 processor computer cluster "Marshall" [5]. The total launched power is the sum over the launched spectrum, typically $-20 < N_\phi < 20$, weighted by the vacuum spectrum and coupling coefficient.

To analyze the density fluctuations measured by the PCI, a synthetic diagnostic has been added to the TORIC post processing. The density fluctuations associated with the RF waves are proportional to the divergence of the perturbed electron velocity, v_{e1}, and v_{e1} can related to the RF electric fields through the linearized electron fluid force balance equation. Using the RF electric fields from TORIC, the 2-D density fluctuations associated with the RF waves can be calculated. These fluctuations can be convolved with PCI instrumental sensitivity and geometry to produce the expected line integrated density fluctuation profile.

To evaluate mode conversion and fast wave current drive scenarios in C-Mod, TORIC is coupled to current drive package based upon Ehst and Karney parameterization of the current drive efficiency [11,12]. This formulation directly includes particle trapping by convolving the local power absorbed with the current drive efficiency at that position. Furthermore, the variation of the parallel wave number is directly accounted because the power absorption is reconstructed as a function of the poloidal mode number. This will be critically important for both the IBW and ICW where the poloidal component of the parallel wave number can dominate the toroidal contribution and result in loss of spectrum control.

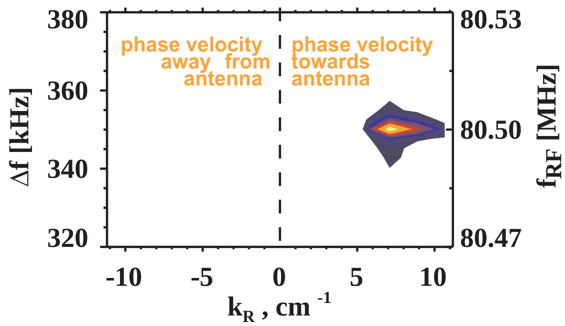

Figure 5: Contour plot of the 2D Fourier transform of the PCI data showing indicating 7 cm^{-1} wavenumber at the expected heterodyne frequency corresponding to RF frequency of 80.5 MHz.

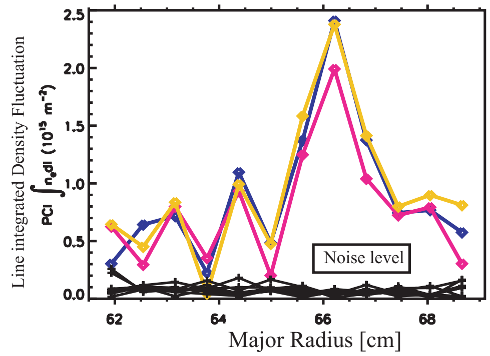

Figure 6: Line integrated PCI signals at the heterodyne frequency before (black) and during RF (color). The magnetic axis is at 67 cm and the mode conversion layer is at 57±2 cm.

3.0 Wave Measurements

The first PCI measurements of the mode conversion region were done for ^{3}He-D-H plasmas for a B_T=5.85 T discharge with an ion mix of 23% ^{3}He, 21% D, 33% H [4]. These measurements utilized FW launch from the nearby D antenna at 80.5 MHz with a vacuum toroidal spectrum peaked at N_ϕ~10. These measurements were the first to confirm the presence of the ICW wave in the plasma core [4]. The TORIC modeling of this scenario was shown in Figure 2. The measured wavenumber and the spatial fluctuation profile relative to the mode conversion layer, shown in Figure 5 and Figure 6, are in agreement with the numerical simulations where the ICW is expected to propagate to the low field side of the mode conversion layer and have a wavenumber ~7 cm^{-1}. The measurements and later simulations demonstrate that due to the large $\boldsymbol{k}_{\|}$ up shift, mode conversion to ICW can be the dominant ICRF mode conversion process.

Using J antenna at 50 MHz, D(^{3}He) plasmas were investigated to simultaneously measure the FW, IBW, and ICW waves in the mode conversion region. A series of L-mode discharges were performed at B_T=5.2, 5.4, and 5.6 T at ~15% ^{3}He concentration thereby moving the mode conversion layer from the high field side (HFS) of the magnetic axis to the low field side (LFS). The line integrated fluctuation data at the heterodyne frequency, $\tilde{n}_{eL} = \int \tilde{n}_e dl$, is shown in Figure 7. Note that in agreement with expectations, the maximum $\tilde{n}_{eL}$ moves towards the LFS as B_T increases. In Figure 8, the contour plot of the 2D Fourier transform of $\tilde{n}_{eL}$ shows the presence of multiple waves. At low k_R(<1 cm^{-1}), both the forward and reflected FW are present. The multiple peaks are a result of the interference pattern associated with the multiple mode converted waves present. This is the first instance where the mode converted waves and the FW have been measured simultaneously in the mode conversion region.

Simple analysis of the local k is difficult because of the multiple waves present. Therefore, the experimental data is compared with a synthetic PCI diagnostic (simulated diagnostic response as calculated from TORIC). A good example of the synthetic and experimental profile comparisons is shown in Figure 9. The agreement between the simulation and the experiment is excellent with respect to the profile shape and the predicted wave number. The comparison of the absolute magnitudes of the fluctuation level is left for future work.

4.0 Mode Conversion Current Drive

Due to the localized nature of the power deposition, mode conversion current drive (MCCD) has the potential to provide local current profile control. For example, as noted previously [13] the rapid up shift of $k_{\parallel}$ of the IBW can in principle result in the degradation of wave directionality because of poloidal up-down asymmetry, thus leading to a loss of current drive efficiency. In the case of current drive by ICW, mode conversion efficiency should be maximized, and particle trapping should be minimized to optimize off-axis current drive efficiency.

The first experimental investigation of MCCD was performed in TFTR [14]. Here the driven current was estimated from a change in loop voltage. The goal of the experiments described below was to experimentally determine the optimum species mix for efficient mode conversion and have the wave in the PCI viewing region. These experiments utilized the J antenna at 78 MHz in D plasmas with a ^{3}He minority. For central deposition, B_T= 8 T, I_p=0.8 MA, and the minority was scanned to maximize the electron deposition. The D antenna operated in heating phase was at 1 MW power level and the J antenna was typically at 1.5 MW. In principle, the driven current could be deduced from the changed in the loop voltage for co- and ctr-current drive phasing. However, the constraints of the experiment resulted in a situation where the fraction of power mode converted was measured to be ~30% of the total injected power or 0.3 MW. From TORIC simulations, the expected driven current was ~10 kA, thus too small to result in significant change in loop voltage. However, the sawtooth behaviour provides a means to infer the presence of a local change in the current profile. The sawtooth period can be lengthened (shortened) by decreasing (increasing) the current gradient at the q=1 surface.[15] As shown in Figure 10, the sawtooth period lengthens to 15 msec for ctr-current drive phasing and shortens to 5 msec for co-current drive phasing. From the

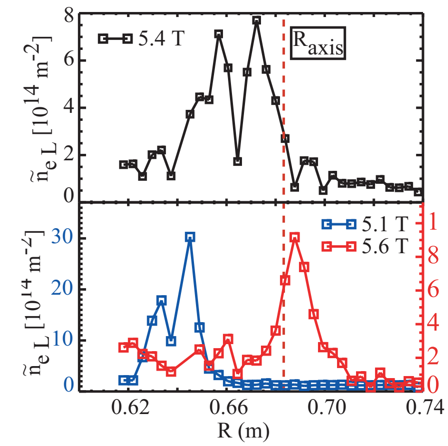

Figure 7: Line integrated fluctuation data at the heterodyne frequency. The spatial profile shifts to larger major radius as the field is increased from 5.1 T to 5.6 T.

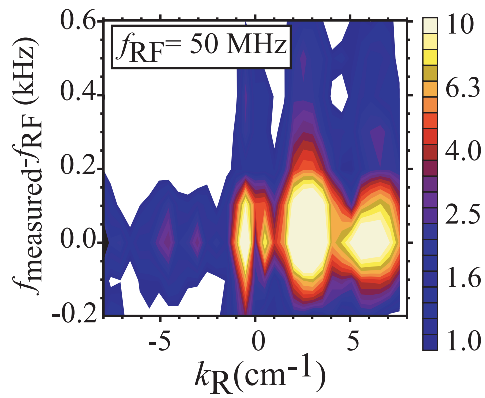

Figure 8: Contour plot of the 2D Fourier transform of the 5.4 T data from Figure 7 showing multiple wave numbers associated at the heterodyne frequency.

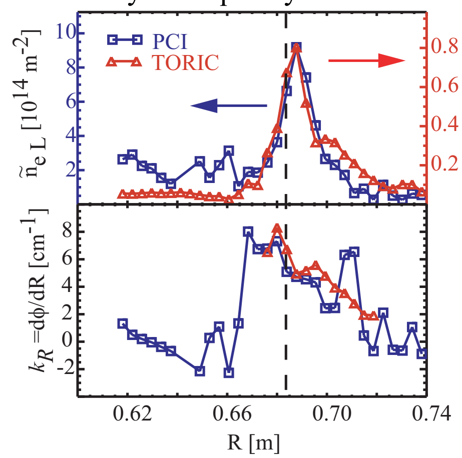

Figure 9: Comparison of the experimental (blue) and synthetic (red) line integrated density fluctuations and local k_R analysis for 5.6 T discharge.

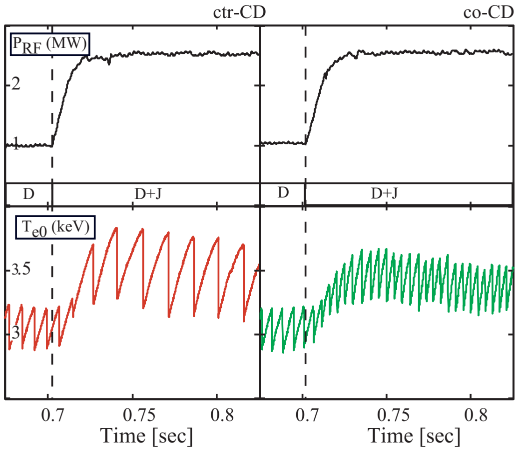

Figure 10: Comparison of the sawtooth behavior for ctr and co-CD phasing.

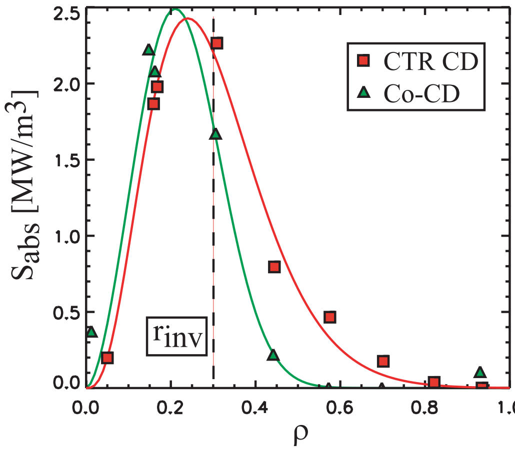

Figure 11: Measured power deposition profile from single RF transition off.

measured power deposition profiles (measured from "break in slope" technique) shown in Figure 11, the deposition profiles for co- and ctr-current drive phasing are similar and the peak of the deposition is just inside the q=1 radius. Furthermore, comparing two ctr-current drive phasing discharges where the deposition is moved from near the q=1 to near axis finds that the near axis deposition does not significantly modify the sawtooth period. This is consistent with a localized driven current near the mode conversion surface.

Using TORIC, simulations have been used to investigate the optimum parameters required to maximize the net driven current and characterize the influence of wave propagation on the driven current (see Figure 12). The simulations show that the driven current by mode converted IBW has a bipolar nature suggesting this branch should be minimized to maximize the net driven current. The ICW and fast wave contribution also has a small off axis reversal resulting from the up down asymmetry in the ICW wave propagation [4,5,6,7]. This result suggests that to maximize the driven current one needs to identify conditions where the ICW branch dominates and is strongly electron Landau damped.

5.0 Mode Conversion Flow Drive

As a result of some ambiguities in the poloidal velocity measurement, the preliminary experiments in three species (D(^{3}He,H)) plasmas at 7.8 T presented in Ref 7 were inconclusive and were recently repeated with improved diagnostics. The mode conversion layer was rather accurately inferred using PCI and the poloidal velocity was measured using a high resolution x-ray spectrometer (HIREX) [16], which measures the Doppler shift of Argon lines. Using two HIREX spectrometers focused upon the same flux surface intersecting the mode conversion layer, the poloidal velocity is measured by subtracting the velocity from the two spectrometers. Although the HIREX is right on the mode conversion layer, no poloidal flow is observed. According to Ref. 6 for flow drive, it is necessary that the MC ICW be damped at the ^{3}He ion cyclotron resonance layer. Therefore, our interpretation of this experiment is in fact that the ICW is too strongly ELD damped and does not reach the low field side ^{3}He ion cyclotron layer. The TORIC simulations of these experiments indicate that most of the mode converted power is damped by electrons. Future experiments will be designed to minimize the electron absorption of the ICW and thereby test theoretical predictions of flow drive.

6.0 Conclusions

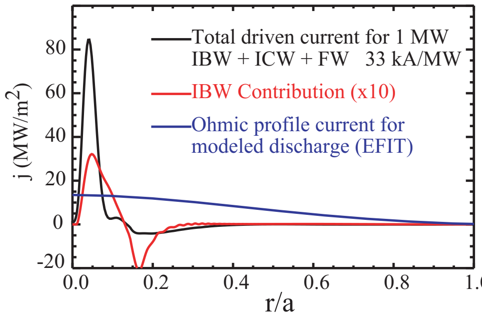

Figure 12: Predicted current profile for mode conversion scenario based upon T_{e0}=5 keV and n_{e0}=$1x10^{20}$.

We reported experimental results on mode conversion processes in multi-ion species plasmas during ICRF experiments in the Alcator C-Mod tokamak at MIT. In addition, we have compared our results with the full wave code, TORIC, predictions. The novel aspect of this work is that we have used a CO_2 laser beam based Phase Contrast Imaging diagnostic (PCI) to monitor the waves in the high temperature and high density core of the C-Mod plasmas. We have successfully measured the dispersion relationship of all waves involved in the mode conversion process, including the Fast Wave, the Ion Bernstein Wave (IBW) and the kinetic electromagnetic Ion Cyclotron Wave (ICW). Our measurements in H-^{3}He plasmas are directly relevant to D-T plasmas in future burning plasma experiments, such as ITER. We have carried out initial experiments on mode conversion current drive and flow drive to test theoretical predictions. While in the initial experiments the current drive powers were too low to detect net current drive, modification of the sawtooth period was clearly observed and was shown to depend on antenna phasing. On the other hand, the results on flow drive experiments were inconclusive. Nevertheless, this is consistent with recent theoretical predictions that flow drive requires absorption of the mode-converted wave on ions rather than electrons which was dominant in these experiments.

7.0 Acknowledgements

We thank the N. Basse and E. Edlund for their help with the PCI diagnostic and the Alcator team for their contributions to these experiments. Work is supported by the Department of Energy Coop. Agreement DE-FC02-99ER54512.

8.0 References

1. T. H. Stix, **Waves in Plasmas,** (Am. Inst. of Physics, New York, 1992).
2. F. W. Perkins, Nucl. Fusion **17**,1197 (1977).
3. M. Porkolab, A. Becoulet, P.T. Bonoli et al., Plasma Phys. Contr. Fusion **40,** A35 (1998).
4. E. Nelson-Melby, M. Porkolab, P.T. Bonoli, et al, Phys. Rev. Lett. **90**, 155004 (2003).
5. J.C.Wright, P.T. Bonoli, M. Brambilla, et al, Phys. Plasmas, **11**, 2473 (2004).
6. E.F. Jaeger et al, Phys. Rev. Lett. **90** ,195001, (2003).
7. Y. Lin, S. Wukitch, P.T. Bonoli, et al, Phys. Plasmas **11**, 2466 (2004).
8. Mazurenko, M. Porkolab, D. Mossessian, et al, Phys. Rev. Lett. **89,** 225004 (2002).
9. S. Coda and M. Porkolab, Rev. Sci. Instrum. **66,** 454 (1995).
10. J.Wright, et al, paper at this conference.
11. P.T. Bonoli et al., Phys. Plasmas **7**, 1886 (2000).
12. D.A. Ehst and C.F. Karney, Nucl. Fusion **31**, 1933 (1991).
13. A. Ram, Proc. of the 11th Top. Conf. on Radio Frequency Power in Plasmas, Palm Springs, CA, A.I.P. Conf. Proc. **355**, 269 (eds. R. Prater and V. Chan), New York (1996).
14. R. Majeski et al., Phys. Rev. Lett. **76**, 764 (1996).
15. Bhatnagar et al., Nucl. Fusion **34**, 1579 (1994).
16. J.E. Rice and E.S. Marmar, Rev. Sci. Instrum. **61**, 2753 (1990).